INTERNATIONAL JOURNAL OF CLIMATOLOGY
Int. J. Climatol. **30**: 1463–1471 (2010)
Published online 3 August 2009 in Wiley InterScience
(www.interscience.wiley.com) DOI: 10.1002/joc.1991

RMetS
Royal Meteorological Society

Atmospheric moisture content associated with surface air temperatures over northern Eurasia

Hengchun Ye[a]* and Eric J. Fetzer[b]

[a] *Department of Geography and Urban Analysis, California State University, 5151 State University Drive, Los Angeles, CA 90032-0882, USA*
[b] *Jet Propulsion Laboratory MS 169-237, California Institute of Technology, 4800 Oak Grove Drive, Pasadena, CA 91109, USA*

ABSTRACT: This study uses both historical station records and Atmospheric Infrared Sounder (AIRS) satellite instrument products to examine the relationship between atmospheric moisture content and surface air temperature over northern Eurasia, with a special emphasis on the summer season. We find that the rate of atmospheric water vapor content change with temperature varies by season and generally decreases with increasing air temperature. The average rate of water vapor pressure increase with air temperature is 7.57%/°C in winter, 4.78%/°C in spring, 3.06%/°C in summer, and 4.39%/°C in fall based on 80 weather station records over a 55-year period. The average rate of atmospheric total precipitable water increases is about 3.02%/°C based on AIRS data from the most recent four summers over northern Eurasia. Except for the winter season, these rates are considerably lower than the 7%/°C rate that the Clausius–Clapeyron relationship and constant relative humidity would suggest. During summer season, we also found decreasing water vapor partial pressure and decreasing total water vapor with increasing air temperature at southern and southwestern study regions where higher mean temperatures are found. The large regional and seasonal variations in water vapor–temperature relationship over Eurasia imply that potential amplified water vapor feedback is most likely to be found in cold regions during the cold season while it may not be as significant as expected during the warm season. Copyright © 2009 Royal Meteorological Society

KEY WORDS atmospheric moisture; northern Eurasia; Clausius–Clapeyron; AIRS; air temperature

Received 3 November 2008; Revised 16 June 2009; Accepted 27 June 2009

1. Introduction

Under conditions of constant relative humidity, atmospheric moisture content increases with air temperature following the Clausius–Clapeyron relationship. The Intergovernmental Panel on Climate Change reports that relative humidity has not shown large changes for the period when instrumental records have been available, and that the average specific humidity increase approximately follows the Clausius–Clapeyron rate of about 7%/°C on the earth's surface (Trenberth *et al*., 2007). In turn, atmospheric cloud cover and the quantity and intensity of precipitation are expected to increase under a warming climate due to the general increase in moisture content (Sun and Groisman, 2000; Semenov and Bengtsson, 2002; Groisman *et al*., 2005; Khon *et al*., 2007). Also, water vapor acts as a greenhouse gas, estimated to account for about 60% of the natural greenhouse effect during periods of clear skies (Kiehl and Trenberth, 1997). This exerts a positive feedback that accelerates atmospheric warming. The nonlinear Clausius–Clapeyron equation predicts that the increase in moisture is significantly larger at higher air temperatures. Consequently, the acceleration of hydrological processes and water vapor-related greenhouse effect would be more evident in summer as long as relative humidity remains roughly constant.

These changes are observed or expected over global scales. Local effects are more complex, and studies have found very large regional variations in the relationship between atmospheric moisture and air temperature (Bauer *et al*., 2002; Trenberth *et al*., 2005; Dai, 2006; Dessler *et al*., 2008). This probably explains different regional trends in precipitation (Dai, 2006). Several studies have found that the most significant increases in land precipitation occurred during winter. For example, increases in winter precipitation/snow accumulation have been documented in northern Eurasia and Canada (Brown and Braaten, 1998; Ye *et al*., 1998; Groisman *et al*., 1999; Serreze *et al*., 2000; Ye, 2001a, b). Increases in high-intensity winter rainfall days were observed in Siberia (Semenov and Bengtsson, 2002; Groisman *et al*., 2005; Khon *et al*., 2007), North America (Karl *et al*., 1998), Switzerland (Schmidli and Frei, 2005), Italy (Brunetti *et al*., 2004), China (Liu *et al*., 2005), and Japan (Easterling *et al*., 2000). In general, most significant increases in precipitation occurred over middle- and high-latitude regions (Huntington, 2006; Trenberth *et al*., 2007).

However, no significant increases, or even decreases, in precipitation were found in lower-latitude land regions,

* Correspondence to: Hengchun Ye, Department of Geography and Urban Analysis, California State University, 5151 State University Drive, Los Angeles, CA 90032-0882, USA.
E-mail: hye2@calstatela.edu

especially during warm seasons (Dai *et al*., 1997, 2004; Trenberth *et al*., 2007). Furthermore, there was no evidence to consistently support the idea that these regions might be subject to an increase in the frequency or intensity of tropical storms and floods (Huntington, 2006). The only exception may be over the tropical oceans, where satellite observations showed an increased frequency in extreme heavy rainfall events but decreases in the frequency of other intensities as sea surface temperature increases (Allan and Soden, 2008). This seems to be consistent with results derived from Global Precipitation Climatology Project products that show precipitation had a positive trend over the tropical ocean but a negative trend over tropical land areas during 1979–2005 (Gu *et al*., 2007). The different trends between tropical ocean and land suggest the possibility that different mechanisms for water vapor cycling and precipitation exist between the two. Few studies have reported significant changes in precipitation during transitional seasons. A recent study by Ye (2008) demonstrated that spring precipitation frequency decreased with increasing air temperature, although winter precipitation frequency increased over northern Eurasia.

The missing evidence of summer warm season precipitation increases with air temperature seems to contradict the water cycle changes we might expect in light of the Clausius–Clapeyron relationship. There are at least two possible explanations: (1) moisture content does increase faster in higher temperature ranges, but the precipitation process is more complex and controlled by the availability of energy; (2) moisture content does not increase as much as expected, or even decreases, in higher temperature ranges due to the scarcity of water sources over land areas in drier regions. A theoretical study by Lindzen (1990) argued that more and deeper convection associated with a warming climate might lead to net drying in certain regions. Is this an indication that the warm season moisture feedback process with temperature has its own regulator, at least in some land regions?

Studies of atmospheric humidity have revealed a general increase with air temperature. Dai (2006) studied the relationship between atmospheric specific humidity and surface air temperature, and suggested that atmospheric moisture content increased with air temperature and that the pattern was very close to what would be predicted by the Clausius–Clapeyron theory. However, there were some tropical and subtropical land regions (South America and many desert regions) where Dai (2006) found that moisture decreased with air temperature instead.

Bauer *et al*. (2002) examined correlations between temperature and water vapor at an interannual time scale of 11 years of radiosondes and climate model reanalysis outputs in different vertical atmospheric layers. They found mostly positive correlations, but also negative ones over certain land areas that are probably related to regional subsidence-related drying and warming of the atmosphere. A recent study using Atmospheric Infrared Sounder (AIRS) data revealed generally positive correlations between specific humidity and air temperature in the lower and upper tropical troposphere, but negative correlation in the middle troposphere (Gambacorta *et al*., 2008). This study also revealed large regional variations, possibly associated with convective ascent and subsidence, although average conditions over the troposphere did follow the Clausius–Clapeyron relationship. A height-varying correlation suggests that relationships revealed by surface observations alone may not accurately reflect the moisture and temperature association over the entire atmospheric column. The large regional variability is also confirmed by Dessler *et al*. (2008)'s study on 5 winters' global relative humidity of AIRS observations. A study by Stephens (1990) of the relationship between monthly mean atmospheric total water vapor and sea surface temperature (SST) over oceans revealed that the relationship resembled the Clausius–Clapeyron curve when the SST was greater than 15 °C, but warned of a potential large difference in the relationship over land areas.

This study examines the relationship between water vapor and surface temperature over Eurasia. Because of its large land mass over high-latitude zones and reasonably long and continuous historical records at weather stations, northern Eurasia has been a focal point for studying potential amplified climate changes over high latitudes. Significant warming and changes in hydrological components are most evident in Eurasian winter and spring (Chapman and Walsh, 1993; Overpeck *et al*., 1997; Serreze *et al*., 2000). Research has mostly dealt with winter precipitation, snow cover/depth, snow season, and river discharges there (Ye *et al*., 1998; Groisman *et al*., 1999; Serreze *et al*., 2000). Little attention has been paid to changes in Eurasian atmospheric water vapor content, which is a key component of not only the hydrological processes, but also the greenhouse feedback process. This study will reveal the seasonal differences in changes in atmospheric moisture content over Eurasia with a focus on the unique characteristics of summer conditions, which may shed some light on the puzzle of warm season climate change over high-latitude land areas.

2. Data and methods

In this research we use both long-term historical synoptic observational records and recently available remote sensing observations. The station records provide 55 years (1936–1990) of detailed historical information for statistical analyses of the near-surface atmosphere. The station data provide surface water vapor partial pressure and air temperature. The remote sensing data are from the AIRS, with product available since 2003 (Chahine *et al*., 2006). This data set allows us to examine the relationship between atmospheric total precipitable water and surface air temperature with a continuous spatial coverage over a more recent time period. The AIRS data serve three important functions: (1) they represent current atmospheric conditions not available from historical station records over the region; (2) total precipitable

water vapor reflects available water vapor over the entire atmospheric column, thus providing valuable information about changes in the relationship between atmospheric moisture content and surface air temperature that is not available from traditional station measurements; (3) continuous spatial coverage across the entire study region that will provide more representative average values for the area.

2.1. Historical station data

The historical station data set used is the Six- and Three-Hourly Meteorological Observations from 223 USSR. Stations available from the Carbon Dioxide Information Analysis Center (CDIAC), Oak Ridge National Laboratory, Oak Ridge, Tennessee (ORNL/CDIAC-180, NDP-048/R1; ftp://cdiac.esd.ornl.gov). Each station record consists of six- (1936–1965) and three-hourly (1966–1990) observations of 24 meteorological variables including air temperature, past and present weather types, precipitation amount, cloud amount and types, sea level pressure, relative humidity, wind speed, and wind direction. The data have undergone extensive quality assurance by the All-Russian Research Institute of Hydrometeorological Information-World Data Centre, the National Climate Data Center, and the CDIAC (Razuvaev *et al*., 1995). The changes in observation times through the two different time periods (before and after 1966) have been adjusted based on station time zone.

To ensure a consistent number of observations per day, only four station observations per day are used throughout the study time period. Thus, for the later period starting in 1966, only the four observations that occurred closest to the previous years' observation times are used. Daily water vapor pressure and air temperature are averaged from the four daily observations. If one observation is missing the day is considered as missing, and if more than 10 days in each month are missing, then the monthly and thus seasonal mean vapor pressure and temperature are considered as missing. There are 80 stations with data starting no later than 1940 and fewer than nine missing years during the period of 1936–1990 that is used for analysis (see Figure 5 for station distribution).

The 55-year seasonal mean water vapor partial pressure is plotted against surface seasonal mean air temperature for all four seasons at all stations to reveal how the relationship compares with the Clausius–Clapeyron curve of saturation vapor pressure for the study region. The calculation of saturation vapor pressure for this curve is based on equations by Riegel (1992) for air temperature above freezing point and below freezing point over water and over ice surface, respectively. The rate of water vapor pressure changes associated with air temperature is calculated based on a simple linear regression with water vapor pressure as the dependent variable and air temperature as the independent variable. The slope of the regression equation is the rate of change for each degree of air temperature increase. When this number is divided by the mean values of the vapor pressure, it becomes the percentage of change per each degree of temperature increase.

Also, vapor pressures are averaged from the five warmest summers (roughly the top 10%), five coldest summers, and the remaining 45 summers for each station to reveal any differences in the relationship of vapor pressure to air temperature for these three categories. This will provide information about extreme as well as normal conditions.

2.2. AIRS water vapor and the gridded surface air temperature data

We use version 5 of AIRS Level 3 total water vapor data in this study. The Level 3 data are gridded 1° latitude by 1° longitude, averaged from the retrieved physical parameters from the Level 2 data that are derived from the radiance data of Level 1 (Granger *et al*., 2004). The AIRS instrument suite consists of a space-based hyperspectral infrared instrument (AIRS) and two multichannel microwave instruments of the Advanced Microwave Sounding Unit and the Humidity Sounders for Brazil. They are some of the instruments onboard the Aqua spacecraft launched 4 May 2002. The atmospheric record from AIRS began in September 2002 and includes high resolution air temperature and humidity profiles, and trace gas amounts for conditions of less than about 70% cloud cover (Chahine *et al*., 2006). Thus the yield decreases with cloud amount, but the retrieval accuracy is independent of cloud amount (Fetzer *et al*., 2006; Susskind *et al*., 2006).

Extensive work has been done on validating AIRS data with the conclusion that AIRS calibrated radiances (Level 1) and retrieved geophysical (Level 2) products generally meet or exceed the prelaunch specifications in Aumann *et al*. (2003) over extrapolar land in the free troposphere, and over extrapolar oceans at all tropospheric altitudes (Chahine *et al*., 2006; Fetzer, 2006; Fetzer *et al*., 2006 and companion articles), and over Antarctica (Gettelman *et al*., 2006; Ye *et al*., 2007).

As with other types of AIRS data, Level 3 has twice-daily values consisting of ascending (north-moving) daytime orbits and descending nighttime orbits. All grid cells covering the geographical area of 0–180 °E, 35–75°N, matching the geographic extent of the weather stations, are selected, and monthly values are averaged from daily values. The daily values are averaged from two orbital overpasses per day, with several individual profiles per overpass in each 1° by 1° cell. If fewer than 20 days are available during a month, the grid cell is considered to have a missing value for that month.

Since the AIRS surface air temperature data have not been specifically validated over the study region, the gridded monthly air temperature data compiled from the historical surface weather station records published by Matsuura and Willmott available from University of Delaware (http://climate.geog.udel.edu/~climate/html_pages/archive.html) Climate Lab are used to study the relationship between total water vapor and surface air temperature. Matsuura and Willmott's data end in 2006,

1 year before the AIRS data. Thus, only four summers are retained for the analyses (2003–2006).

The 4-year mean total water vapor is plotted against the surface air temperature for all grids. The averaged values of total water based on each one-degree increment of air temperature are compared to that of the Clausius–Clapeyron line. The rate of change in total precipitable water associated with surface air temperature is calculated in the same way as the station data described above.

3. Results

3.1. Station records of surface temperature and water vapor pressure

The scatter plot of seasonal mean water vapor pressure *versus* air temperature for the 80 stations during 1936–1990 is shown in Figure 1. The vapor pressure increases with air temperature in general for all seasons; however, the observations do not closely follow the Clausius–Clapeyron line except for the winter season. The largest deviations occur in summer when vapor pressures are all below the Clausius–Clapeyron value. Since the Clausius–Clapeyron line represents the saturation vapor pressure associated with increasing air temperature, the stations' vapor pressures should be lower if the relative humidity is below 100%. The pattern of general increase should follow this saturation line with a slightly gentler slope depending on relative humidity conditions. However, the summer mean vapor pressure reaches a maximum of about 17.5 hPa at a mean air temperature of about 19 °C. For stations with summer mean air temperature higher than 20 °C, vapor pressure falls below 15 hPa. For a closer look at the summer relationship, the mean vapor pressure values for the five hottest, five coldest, and the remaining 45 summers are plotted

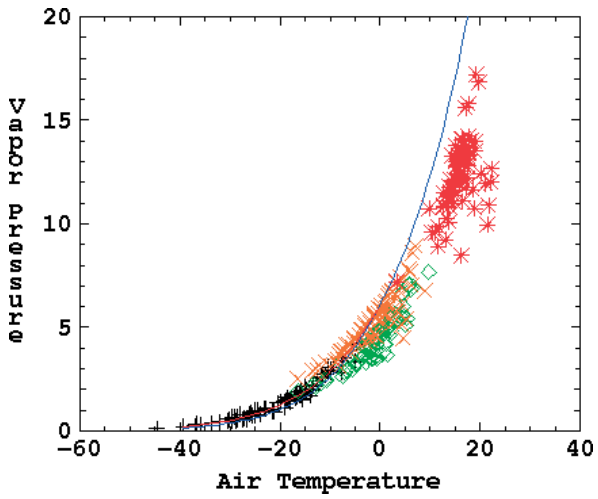

Figure 1. Mean seasonal vapor pressure *versus* air temperature at 80 stations for winter (black plus), spring (green diamond), summer (red star), and fall (orange cross) averaged for the time period of 1936–1990. Thin solid line is the Clausisus–Clapeyron line of saturation vapor pressure.

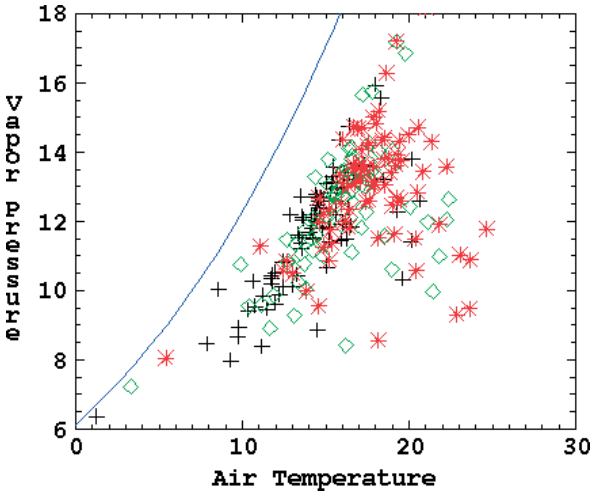

Figure 2. Scatter plot of mean summer vapor pressure *versus* temperature for five lowest temperature summers (black-cross) and five highest temperature summers (red-star), and the remainder (green diamond) based on 1936–1990.

against the corresponding summer air temperatures for all stations in Figure 2. It is clear from this figure that the five hottest summers, with mean temperatures of 22 to 25 °C have vapor pressures of only 9 to 12 hPa. In contrast, in the coldest summer category the highest mean summer vapor pressure is 17.5 hPa at a mean summer temperature of about 19 °C, the same maximum value as for the 45 summers in the middle-temperature-range category. More stations in the hottest summer category (red asterisks in Figure 2) have lower vapor pressures than the other two categories of coldest and middle-range summers. Therefore, highest summer air temperatures are consistently associated with lower vapor pressures. Similarly, the coldest summer category (blue crosses) has the fewest stations showing decreasing vapor pressures with increasing air temperature. Figure 2 suggests that as air temperature continues to increase with increasing greenhouse forcing, water vapor pressure may decrease rather than increase over high-latitude land areas.

The amplitudes of seasonal vapor pressure change per degree of air temperature increase during the 55-year study period for all 80 stations are shown in Figure 3. As expected, the amount of vapor pressure increases as air temperature increases, with larger increases in the higher temperature range in the winter season. Spring and fall show a spread in the amount of increase for increasing temperature. For summer, the amount of vapor pressure increase becomes smaller and shifts abruptly to a decrease at stations with mean summer air temperature at around 20 °C and higher. When the rate of change is divided by its corresponding station's mean vapor pressure, the percentage of rate change decreases with air temperature (Figure 4). In general, it is clear that the percentage of rate of change decreases with increasing air temperature in all seasons. Winter has the highest rate of change, ranging from about 5 to 14.5%/°C with an average value of about 7.57%/°C among these 80 stations (Figure 4). The spring and fall have an average of about 4.8%/°C

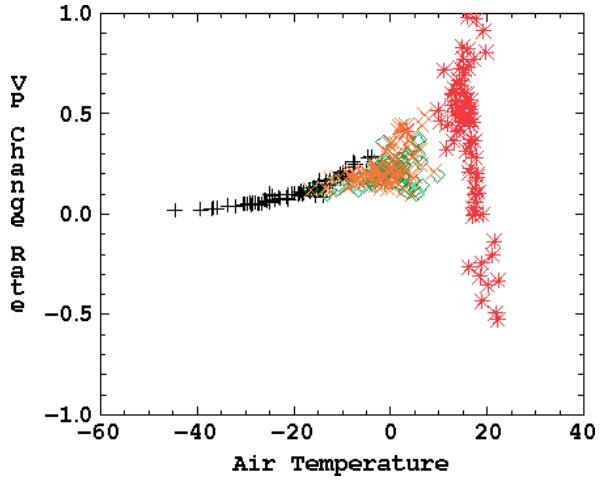

Figure 3. The amount of vapor pressure change with each degree of air temperature increase (hPa/°C) *versus* mean air temperatures for 80 stations for winter (black plus), spring (green diamond), summer (red star), and fall (orange cross) based on 1936–1990.

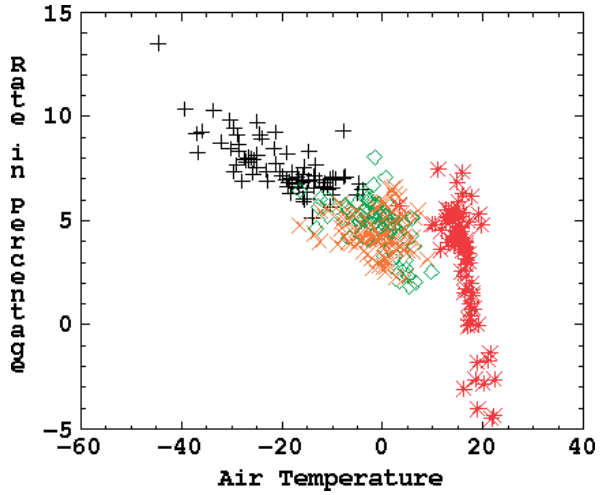

Figure 4. The same as Figure 3, but for percentage of changes in vapor pressure.

and 4.4%/°C, respectively. The summer has the largest variation among stations, ranging from −5 to 7.5%/°C, and the higher values are at stations with lower mean summer air temperatures. The average change rate for all 80 stations is 3.06%/°C. Figure 4 suggests that the rates of change in vapor pressure based on the 55-year study period are in general lower than 7%/°C based on the Clausius–Clapeyron theory, except for the winter season when they are slightly higher instead. In light of the large deviation of summer water vapor change rates from those that the theory predicts, the rest of the article will focus on the summer season to further reveal the geographical characteristics of this relationship.

Figure 5 maps the locations of the summer temperature categories having highest mean vapor pressures. Ten stations located along a 50–60°N belt (red in Figure 5) have highest vapor pressures occurring in the coldest category, suggesting warmer temperatures are associated

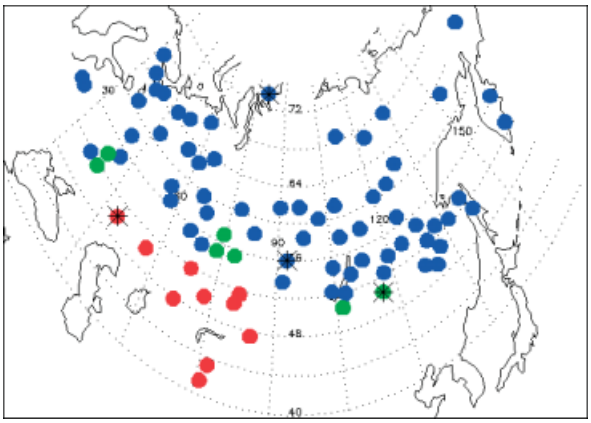

Figure 5. The category of air temperature corresponding to the highest mean vapor pressure based on the 55 years of study period. Blue: the highest air temperature category having the highest mean vapor pressure; Green: the middle temperature category having the highest vapor pressure; red: the coldest category having the highest mean vapor pressure. Stars indicate stations that are used in Figure 6.

with lower vapor pressures. Moving northward, six stations (in green in Figure 5) have highest vapor pressures in the middle category. These 16 stations provide evidence for decreasing vapor pressure with air temperature during the study time period of 1936–1990. Among these 16 stations, 12 have a negative correlation of vapor pressure with air temperature, and 7 of these are statistically significant (not shown). Only the highest latitude stations show the increase in vapor pressure with temperature during warm summers (blue in Figure 5) expected from constant relative humidity and the Clausius–Clapeyron relationship. The geographical distribution of the varying relationships corresponds broadly to the surface biomes, with negative relationships in grassland and positive ones over taiga regions. This may suggest that grassland soils dry more easily and that lower evapotranspiration leads to lowered atmospheric moisture content during hot summers.

All these figures show a consistent pattern of relationships between mean summer vapor pressure and air temperature at individual stations: vapor pressure increases with air temperature, but then decreases as air temperature increases above a threshold value. It appears that the transitions occur at temperatures of about 14–20 °C depending on the locations, except for a few stations in the southwest part of the study region where vapor pressure decreases with temperature throughout most years. These stations already have higher mean temperatures. Figure 6 illustrates four selected stations with varying transition temperature ranges. The station at Ostrov Dikson (73.5 °N, 80.40 °E, elevation 42 m) shows no decrease in vapor pressure with temperature. The air temperature there is very low, below 6 °C. The station at Krasnojarsk (56.0 °N, 92.88 °E, elevation 274 m) shows decreasing vapor pressure starting at a temperature of about 17.5 °C. The decrease starts at a temperature of about 18.5 °C for the station at Borzja

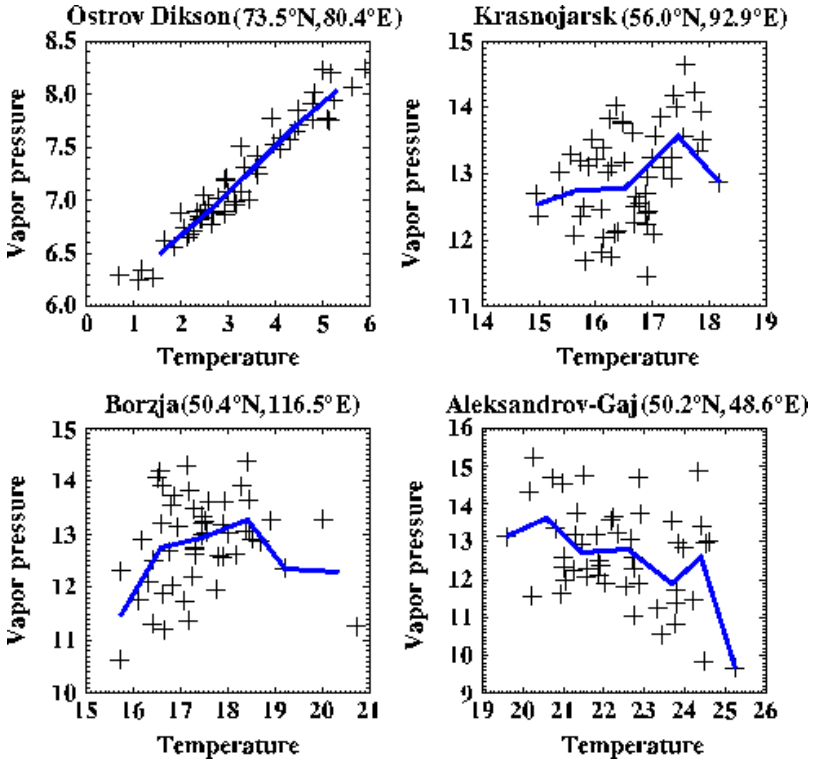

Figure 6. Vapor pressure *versus* air temperature at four selected stations during 1936–1990. Thick solid line is the averaged vapor pressure based on the 0.5 °C increment in temperature. This figure is available in colour online at www.interscience.wiley.com/ijoc

(50.38 °N, 116.52 °E, elevation 675 m) and vapor pressure seems to start decreasing at a temperature of 20 °C in Aleksandrov-Gaj (50.15 °N, 48.55 °E, elevation 23 m). Of course, the transition temperature illustrated here depends on these 55 years of data and at certain stations there are not enough high temperature summers to robustly support the idea of a threshold temperature for transition. Also, worth noting is a much wider spread of vapor pressure values at higher temperature stations in Figure 6. For example, vapor pressure can vary from 10 to 15 hPa at air temperatures of around 24 °C while it ranges from 7.7 to 8.2 hPa at temperatures of about 5 °C. The largest range of vapor pressure among these four stations is at the warmest station of Aleksandrov-Gaj (Figure 6).

3.2. AIRS total water vapor and surface air temperature

The AIRS 4-year mean summer total vapor *versus* summer air temperature for all grids over the study region in Figure 7 shows that grids with higher air temperatures have higher total vapor, until the temperature reaches 25 °C. Above 25 °C, total vapor has lower mean values and larger variability. The thick line (averaged total vapor at each 1 °C increment) crosses the thin line (Clausius–Clapeyron curve) showing higher total vapor at lower air temperatures and lower vapor at higher temperatures on average. This also shows a lower rate of increase in total vapor, and eventual decreases at higher air temperatures.

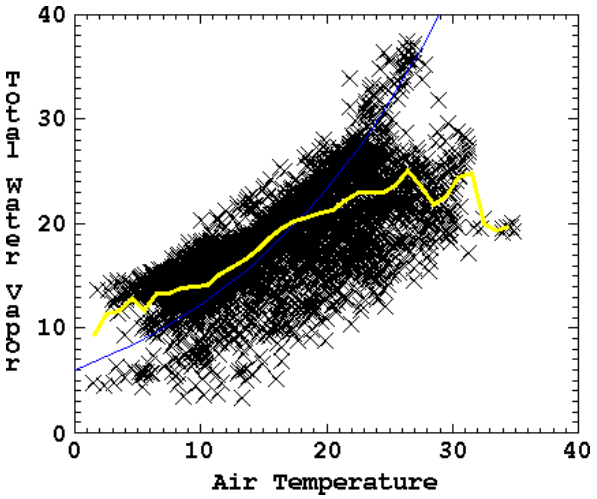

Figure 7. Mean summer total water vapor *versus* air temperature for all grids over northern Eurasia for 2003–2006. Thin line: Clausius–Claperyon relationship of saturation vapor pressure; Thick line: average total water vapor for grids with each increment of air temperature. This figure is available in colour online at www.interscience.wiley.com/ijoc

The distribution of total water change *versus* air temperature in Figure 8 ranges from −0.5 mm to 1.5 mm/°C over the study region for the four summers of 2003–2006. There is also a general tendency for a slight decreasing in magnitude of water vapor change as air temperatures increase. When the percentage of change rate is used, the downward trend towards higher air temperatures becomes more evident (Figure 9). The rate of change varies from

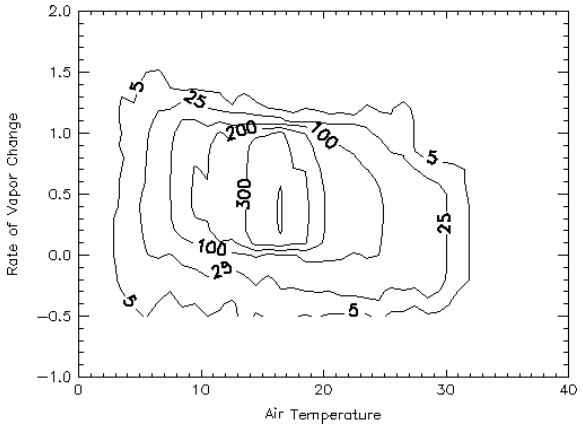

Figure 8. Plot of total precipitable water vapor change (mm/°C) *versus* air temperature averaged over 2003–2006 summers over northern Eurasia. The contours are the total number of grids corresponding to the total precipitable water vapor change and mean summer air temperature values.

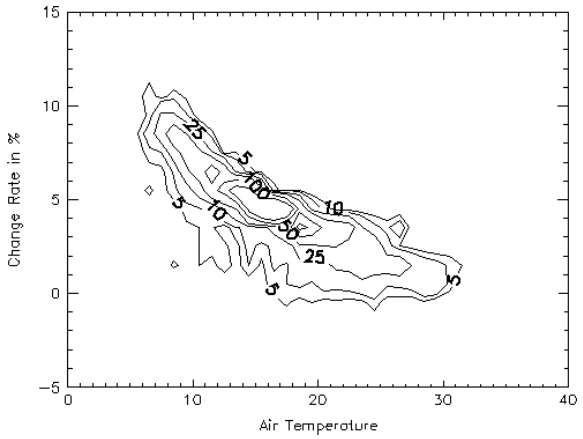

Figure 9. The same as Figure 8, but for the percentage of rate of water vapor change (%/°C).

−4.75 to 27.55%/°C with the majority of AIRS grid cells having values of around 4 to 5%/°C. This again suggests that grids with higher air temperatures have lower rates of change in total water vapor.

The geographical distribution of the percentage of rate change of total water vapor with temperature in the AIRS data is shown in Figure 10. It is evident that near zero and negative rates of change are located at low-latitude regions while positive rates are found over northern regions. This pattern resembles Figure 5 for the station data. The area-averaged change rate for all grids (by using square root of cosine latitude to adjust for the changes in grid sizes) is 3.02%/°C over the study region. These warmer lower-latitude regions again coincide with grasslands, and cooler higher latitude regions with taiga forest. The weak and negative relationships between vapor and air temperature may partially be due to quicker drying of soil moisture in grasslands compared to forest areas, thus reducing evapotranspiration and atmospheric water vapor.

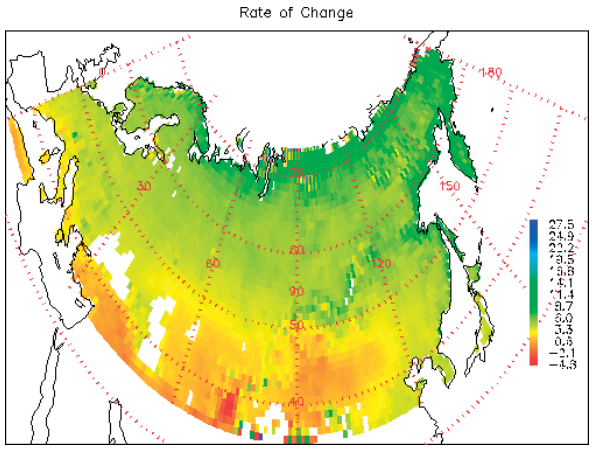

Figure 10. Distribution of rate of change of total precipitable water (%/°C).

4. Summary and conclusions

This study uses both historical station records and remote sensing products to examine the relationships between atmospheric moisture and surface air temperature over northern Eurasia. The results show that the rate of atmospheric water vapor change over the study region does not stay constant, but rather decreases with increasing air temperature in general. The highest rates of increase with temperature occur in winter, with lowest rates in summer. The water vapor change with air temperature is consistent with Clausius–Clapeyron only in winter, with an average of 7.57%/°C. All other seasons have lower rates of increase. The average rate of water vapor increase over northern Eurasia during summer is about 3.06%/°C (based on 80 stations during 55 years of records) for vapor pressure and 3.02%/°C for total precipitable water based on almost the entire study region (from the satellite data) for the four recent summers. Furthermore, it appears that the rates of change decrease and even switch to negative values when air temperatures exceed about 25 °C. This smaller rate of increase has also been observed by Kay *et al.* (2008) in a study of the western Arctic, where air temperature increases outpaced moisture increases during the summer of 2007. Results indicate that the Clausius–Clapeyron theory of increasing atmospheric moisture with increasing air temperature only appears to hold in the northern part of the study region during summer, where lower temperatures predominate. This is consistent with other results showing that the relationship between atmospheric vapor content and air temperature varies geographically, at least at regional scales. The strong temperature dependence of the moisture change rate found in this study implies that vapor feedback may not be as strong as would be expected by Clausius–Clapeyron and constant relative humidity, or may even be dampened, in warm regions and/or during the warm season. However, it would be strengthened in colder regions and/or during the cold season if the hemispheric-mean conditions followed the Clausius–Clapeyron relationship.

The cause for the small or even negative rates of change in moisture for higher air temperature conditions in the southern and southwestern parts of the study region may be drying of soil moisture over grasslands, and thus reduced local evaporation plus less transpiration compared to forest land cover. In a study of atmospheric moisture over Europe Zveryaev *et al*. (2008) suggest that horizontal moisture transport in summer is minimal and that local processes dominate moisture variations. This is also suggested by Numaguti (1999) who specifically suggests that the main source of summer precipitable water is local evaporation over the Eurasian continent. Trenberth *et al*. (2003) also suggested that increasing atmospheric water vapor associated with increasing air temperature is primarily through evaporation. If surface soil dries after a long spell of high temperatures, it is likely that evaporation decreases, resulting in decreased atmospheric water vapor. To further verify this, a water budget analysis would be employed to examine those days with high soil moisture deficits to compare their atmospheric moisture conditions on other days. We have looked into the possible shift in wind directions that might have caused drier and hotter summers, but results are inconclusive due to the fact that different stations have differing wind directions associated with the increasing air temperatures. Analyses on changes in frequency and intensity of warm, dry air masses, and changes in air pressure and cyclonic activity may reveal their impact on the drying of soil moisture. Similar studies could be applied to other land areas, especially to include lower-latitude regions in order to draw a more complete picture of the geographical and seasonal patterns of these relationships. Identifying the geographical regions where temperature-dependent dehydration occurs is important to understanding changing precipitation properties under a warming climate over land areas.

Acknowledgements

The first author would like to thank JPL's summer faculty fellowship and the CEA-CREST program at Cal-State LA for making this research possible. The second author was supported by the AIRS project at JPL, and by the NASA and Energy and Water-cycle Study (NEWS) project. Part of the research described in this paper was carried out at the Jet Propulsion Laboratory, California Institute of Technology, under a contract with the National Aeronautics and Space Administration.

References

Allan RP, Soden BJ. 2008. Atmospheric Warming and the Amplification of Precipitation Extremes. *Science* **321**(5895): 1481–1484.

Aumann HH, Chahine MT, Gautier C, Goldberg MD, Kalnay E, McMillin LM, Revercomb H, Rosenkranz PW, Smith WL, Staelin DH, Strow LL, Susskind J. 2003. AIRS/AMSU/HSB on the Aqua mission: Design, science objectives, data products, and processing systems. *IEEE Transactions on Geoscience and Remote Sensing* **41**(2): 253–264.

Bauer M, Del Genio AD, Lanzante JR. 2002. Observed and simulated temperature-humidity relationships: sensitivity to sampling and analysis. *Journal of Climate* **15**: 203–215.

Brown RD, Braaten RO. 1998. Spatial and temporal variability of Canadian monthly snow depths, 1946–1995. *Atmosphere-Ocean* **36**: 37–54.

Brunetti M, Maugeri M, Monti F. 2004. Changes in daily precipitation frequency and distribution in Italy over the last 120 years. *Journal of Geophysical Research* **109**: D05102, DOI:10.1029/2003JD004296.2004.

Chahine MT, Pagano TS, Aumann HH, Atlas R, Barnet C, Blaisdell J, Chen L, Divakarla M, Fetzer EJ, Goldberg M, Gautier C, Granger S, Hannon S, Irion FW, Kakar R, Kalnay E, Lambrigtsen BH, Lee SY, Le Marshall J, McMillan WW, McMillin L, Olsen ET, Revercomb H, Rosenkranz P, Smith WL, Staelin D, Strow LL, Susskind J, Tobin D, Wolf W, Zhou LH. 2006. AIRS: Improving weather forecasting and providing new data on greenhouse gases. *Bulletin of the American Meteorological Society* **87**(7): 911–926.

Chapman WL, Walsh JE. 1993. Recent variations of sea ice and air temperature in high latitudes. *Bulletin of the American Meteorological Society* **74**: 33–47.

Dai A. 2006. Recent climatology, variability, and trends in global surface humidity. *Journal of Climate* **19**(15): 3589–3606.

Dai A, Fung IY, Delgenio AD. 1997. Surface observed global land precipitation variations during 1900–1988. *Journal of Climate* **10**: 2943–2962.

Dai A, Lamb PJ, Trenberth KE, Hulme M, Jones PD, Xie P. 2004. The recent Sahel drought is real. *International Journal of Climatology* **24**: 1323–1331.

Dessler AE, Yang P, Zhang Z. 2008. Water-vapor climate feedback inferred from climate fluctuations. *Geophysical Research Letters* **35**: L20704, DOI:10.1029/2008GL035333.

Easterling DR, Evans JL, Groisman PY, Karl TR, Kunkel KE, Amebenje P. 2000. Observed variability and trends in extreme climate events: a brief review. *Bulletin of the American Meteorological Society* **81**: 417–425.

Fetzer EJ. 2006. Preface to special section: validation of atmospheric infrared sounder observations. *Journal of Geophysical Research* **111**: DOI:10.1029/2005JD007020.

Fetzer EJ, Lambrigtsen BH, Eldering A, Aumann HH, Chahine MT. 2006. Biases in total precipitable water vapor climatologies from Atmospheric Infrared Sounder and Advanced Microwave Scanning Radiometer. *Journal of Geophysical Research* **111**: D09S16, DOI:10.1029/2005JD006598.

Gambacorta A, Barnet C, Soden B, Strow L. 2008. An assessment of tropical humidity-temperature covariance using AIRS. *Geophysical Research Letters* **35**: L10814, DOI:10.1029/2008GL033805.

Gettelman A, Walden VP, Miloshevich LM, Roth WL, Halter B. 2006. Relative humidity over the Antarctic from radiosonde, satellite, and a general circulation model. *Journal of Geophysical Research* **111**: D09513, DOI:10.1029/2005JD006636.

Granger S, Leroy SS, Manning EM, Fetzer EJ, Oliphant RB, Braverman A, Lee SY, Lambrigtsen B. 2004. Development of level 3 (gridded) products for the Atmospheric Infrared Sounder (AIRS), in *Proceedings of IGARSS 2004*, 20–24 September 2004, Anchorage Alaska.

Groisman PY, Karl TR, Easterling DR, Knight RW, Jamason PF, Hennessy KJ, Suppiah R, Page CM, Wibig J, Fortmiak K, Razuvaev VV, Douglas A, Førland EJ, Zhai P. 1999. Changes in the probability of heavy precipitation: important indicators of climatic change. *Climatic Change* **42**: 243–283.

Groisman PY, Knight RW, Easterling DR, Karl RT, Hegerl GC, Razuvaev VN. 2005. Trends in intense precipitation in the climate record. *Journal of Climate* **18**: 1236–1251.

Gu G, Adler RF, Huffman GJ, Curtis S. 2007. Tropical rainfall variability on interannual-to-interdecadal and longer time scales derived from the GPCP monthly product. *Journal of Climate* **20**: 4033–4046.

Huntington TG. 2006. Evidence for intensification of the global water cycle: review and synthesis. *Journal of Hydrology* **319**(1–4): 83–95.

Intergovernmental Panel on Climate Change. 2007. Summary for policymakers. In *Climate Change 2007: The Physical Science Basis. Contribution of Working Group I to the Fourth Assessment Report of the Intergovernmental Panel on Climage Change*, Solomon S, Qin D, Manning M, Chen Z, Marquis M, Averyt KB, Tignor M, Miler HL (eds). Cambridge University Press: Cambridge, New York.

Karl TR, Knight RW. 1998. Secular trends of precipitation, frequency, and intensity in the United States. *Bulletin of the American Meteorological Society* **79**: 231–241.

Kay JE, L'Ecuyer T, Genttelman A, Stephens G, O'Dell C. 2008. The contribution of cloud and radiation anomalies to the 2007 Arctic

sea ice extent minimum. *Geophysical Research Letters* **35**: L08503, DOI:10.1029/2008GL033451.

Khon VCh, Mokhov II, Roeckner E, Semenov VA. 2007. Regional changes of precipitation characteristics in northern Eurasia from simulations with global climate model. *Global and Planetary Change* **57**(1/2): 118–123.

Kiehl JT, Trenberth KE. 1997. Earth's annual global mean energy budget. *Bulletin of the American Meteorological Society* **78**: 197–208.

Lindzen RS. 1990. Some coolness concerning global warming. *Bulletin of American Meteorology Society* **71**(3): 288–299.

Liu B, Xu M, Henderson M, Ye Q. 2005. Observed trends of precipitation amount, frequency, and intensity in China, 1960–2000. *Journal of Geophysical Research* **110**: D08103, DOI:10.1029/2004JD004864.

Numaguti A. 1999. Origin and recycling processes of precipitating water over the Eurasian continent: experiments using an atmospheric general circulation model. *Journal of Geophysical Research* **104**: 1957–1975.

Overpeck J, Hughen K, Hardy D, Bradley R, Case R, Douglas M, Finney M, Gajewski K, Jacoby G, Jennings A, Lamoureux S, Lasca A, MacDonald G, Moore J, Retelle M, Smith S, Wolfe A, Zielinski G. 1997. Arctic environmental change of the last four centuries. *Science* **278**: 1251–1256.

Razuvaev VN, Apasova EB, Martuganov RA. 1995. *Six- and Three-hourly Meteorological Observations from 223 U.S.S.R. Stations. NDP-048/R1*. Carbon Dioxide Information Analysis Center, Oak Ridge National Laboratory: Oak Ridge.

Riegel CA. 1992. *Fundamentals of Atmospheric Dynamics and Thermodynamics*, Bridger AFC (eds). World Scientific Publishing: New Jersey; p 496.

Schmidli J, Frei C. 2005. Trends of heavy precipitation and wet and dry spells in Switzerland during the 20th century. *International Journal of Climatology* **25**: 753–771.

Semenov VA, Bengtsson L. 2002. Secular trends in daily precipitation characteristics: greenhouse gas simulation with a coupled AOGCM. *Climate Dynamics* **19**: 123–140.

Serreze MC, Walsh JE, Chapin FS III, Osterkamp T, Dyurgerov M, Romanovsky V, Oechel WC, Morison J, Zhang T, Barry RG. 2000. Observational evidence of recent changes in the northern high-latitude environment. *Climatic Change* **6**: 159–208.

Stephens GL. 1990. On the relationship between water vapor over the oceans and sea surface temperature. *Journal of Climate* **3**: 634–645.

Sun B, Groisman PY. 2000. Cloudiness variations over the former Soviet Union. *International Journal of Climatology* **20**: 1097–1111.

Susskind J, Barnet C, Blaisdell J, Iredell L, Keita F, Kouvaris L, Molnar G, Chahine M. 2006. Accuracy of geophysical parameters derived from Atmospheric Infrared Sounder/Advanced Microwave Sounding Unit as a function of fractional cloud cover. *Journal of Geophysical Research* **111**(D9): D09S17, DOI:10.1029/2005JD006272.

Trenberth KE, Dai A, Rasmussen RM, Parsons DB. 2003. The changing character of precipitation. *Bulletin of American Meteorology Society* **84**: 1205–1217.

Trenberth K, Fasullo J, Smith L. 2005. Trends and variability in column-integrated atmospheric water vapor. *Climate Dynamics* **24**: 741–758.

Trenberth KE, Jones PD, Ambenje P, Bojariu A, Easterling D, Klein A, Tank D, Dark D, Rahimzadeh F, Renwick JA, Rusticucci M, Soden B, Zhai P. 2007. Observations: surface and atmospheric climate change. In: *Climate Change 2007: The Physical Science Basis. Contribution of Working Group I to the Fourth Assessment Report of the Intergovernmental Panel on Climate Change*, Solomon S, Qin D, Manning M, Chen Z, Marquis M, Averyt KB, Tignor M, Miller HL (eds). Cambridge University Press: Cambridge, New York.

Ye H. 2001a. Characteristics of winter precipitation variation over northern Eurasia and their connections to sea surface temperatures over the Atlantic and Pacific Oceans. *Journal of Climate* **14**: 3140–3155.

Ye H. 2001b. Quasi-biennial and quasi-decadal variations in snow accumulation over northern central Eurasia and their connections to Atlantic and Pacific Oceans and Atmospheric circulation. *Journal of Climate* **4**: 4573–4584.

Ye H. 2008. Changes in precipitation types associated with surface air temperature during 1936-90 over northern Eurasia. *Journal of Climate* **21**: 5807–5819.

Ye H, Cho H, Gustafson P. 1998. The changes of Russian winter snow accumulation during 1936–1983 and its spatial patterns. *Journal of Climate* **11**: 856–863.

Ye H, Fetzer EJ, Bromwich DH, Fishbein EF, Olsen ET, Granger SL, Lee S, Chen L, Lambrigtsen BH. 2007. Atmospheric total precipitable water from AIRS and ECMWF during Antarctic summer. *Geophysical Research Letters* **34**: L19701, DOI:10.1029/2006GL02854.

Zveryaev II, Wibig J, Allan RP. 2008. Contrasting interannual variability of atmospheric moisture over Europe during cold and warm seasons. *Tellus* **60A**: 3–41.

